Naphthalenones from a Perenniporia sp Inhabiting the Larva of a Phytophagous Weevil, Euops chinesis

ARTICLE *in* JOURNAL OF NATURAL PRODUCTS · JUNE 2012

Impact Factor: 3.8 · DOI: 10.1021/np300263u · Source: PubMed

7 AUTHORS, INCLUDING:

Shubin Niu
Beijing City University
37 PUBLICATIONS **259** CITATIONS
SEE PROFILE

Li Li
Guangxi Medical University
560 PUBLICATIONS **8,557** CITATIONS
SEE PROFILE

Xingzhong Liu
Chinese Academy of Sciences
223 PUBLICATIONS **2,245** CITATIONS
SEE PROFILE

Yongsheng Che
Beijing institute of Pharmacology & Toxicology
91 PUBLICATIONS **967** CITATIONS
SEE PROFILE

JOURNAL OF NATURAL PRODUCTS

Article

pubs.acs.org/jnp

Naphthalenones from a *Perenniporia* sp. Inhabiting the Larva of a Phytophagous Weevil, *Euops chinesis*

Yu Feng,[†,‡,§] Lin Wang,[†,‡,§] Shubin Niu,[†] Li Li,[⊥] Yikang Si,[⊥] Xingzhong Liu,*[,†] and Yongsheng Che*[,†,∥]

[†]State Key Laboratory of Mycology, Institute of Microbiology, Chinese Academy of Sciences, Beijing 100190, People's Republic of China

[‡]Graduate School of Chinese Academy of Sciences, Beijing 100039, People's Republic of China

[⊥]Institute of Materia Medica, Chinese Academy of Medical Sciences and Peking Union Medical College, Beijing 100050, People's Republic of China

[∥]Beijing Institute of Pharmacology & Toxicology, Beijing 100850, People's Republic of China

Supporting Information

ABSTRACT: The new naphthalenone derivatives perenniporides A–D (**1**–**4**) were isolated from solid cultures of a fungus *Perenniporia* sp. inhabiting the larva of *Euops chinesis*, a phytophagous weevil with high host specificity to the medicinal plant *Fallopia japonica*. The structures of **1**–**4** were elucidated primarily by NMR experiments, and **1** was confirmed by X-ray crystallography. The absolute configuration of **1** and **2** was assigned by electronic circular dichroism (ECD) calculations, whereas that of the C-10 tertiary alcohol in **3** was deduced via the CD data of the *in situ* formed $[Rh_2(OCOCF_3)_4]$ complex and supported by the ECD data. Compound **1** showed antifungal activity against five plant pathogens.

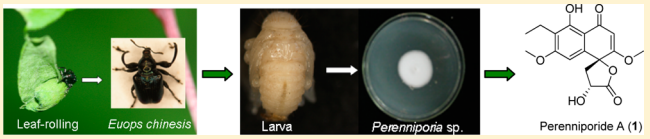

Euops chinesis is a phytophagous attelabid weevil with high host specificity to the traditional medicinal plant *Fallopia japonica*.[1] The female weevils make leaf-roll cradles in which the eggs are laid and the larva develops while feeding on the cradles.[1] During our ongoing search for new bioactive natural products from fungi of unique niches,[2] a strain of *Perenniporia* sp. was chemically investigated. *Perenniporia* is a mostly perennial genus found on dead and living hardwood and conifers.[3] To date, only a few bioactive secondary metabolites have been isolated from the species of this genus including pereniporins A and B,[4] perenniporiol derivatives,[5,6] and antibiotic 8345 C.[7] In the current work, the fungus was initially found in the larva of *E. chinesis* that was collected from Mingyue Mountain, Jiangxi Province, People's Republic of China, and subsequently isolated from the leaves of the medicinal plant *F. japonica*. To our knowledge, a variety of natural products have been isolated from *F. japonica*. Examples include anthraquinones,[8,9] stilbenes,[10,11] phenols,[9] flavonoids,[12] and other compounds such as 2-methoxy-6-acetyl-7-methyljuglone.[9] Fractionation of an EtOAc extract prepared from a solid-substrate fermentation of the fungus afforded four new naphthalenone derivatives, named perenniporides A–D (**1**–**4**), and the known compound 6-ethyl-2,7-dimethoxyjuglone (**5**).[13] Compound **5** is closely related to 2-methoxy-6-acetyl-7-methyljuglone,[9] which was isolated from the medicinal plant *F. japonica*. Details of the isolation, structure elucidation, and antifungal activity of **1**–**4** are reported herein.

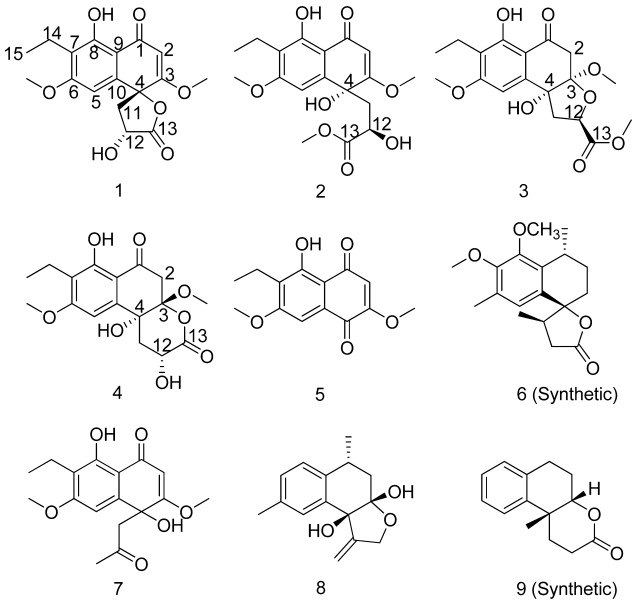

RESULTS AND DISCUSSION

Perenniporide A (**1**) was assigned the molecular formula $C_{17}H_{18}O_7$ (nine degrees of unsaturation) on the basis of HRESIMS. Analysis of its ^1H and ^{13}C NMR data (Table 1) revealed two exchangeable protons (δ_H 5.30 and 13.14, respectively), three methyl groups including two *O*-methyls, two methylenes, one *O*-methine, eight olefinic/aromatic carbons (two of which were protonated), one oxygenated sp^3 quaternary carbon, one carboxylic carbon (δ_C 176.9), and one

Received: April 10, 2012
Published: June 25, 2012

Table 1. NMR Data for 1 and 2

	1			2		
pos.	δ_C,[a] mult.	δ_H[b] (J in Hz)	HMBC[a]	δ_C,[c] mult.	δ_H[d] (J in Hz)	HMBC[c]
1	190.0, qC			189.7, qC		
2	101.4, CH	5.77, s	1, 3, 4, 9	100.9, CH	5.63, s	1, 3, 4, 9
3	173.8, qC			177.3, qC		
4	78.6, qC			70.7, qC		
5	101.5, CH	6.81, s	1, 4, 6, 7, 9, 10	100.9, CH	6.79, s	4, 6, 7, 9, 10
6	163.6, qC			161.7, qC		
7	120.2, qC			116.9, qC		
8	161.0, qC			159.2, qC		
9	108.6, qC			108.1, qC		
10	142.5, qC			146. 4, qC		
11	47.7, CH_2	3.17, dd (14.0, 9.5); 2.50, dd (14.0, 9.0)	3, 4, 10, 12, 13	47.7, CH_2	2.55, m; 209, m	3, 4, 10, 12, 13
12	68.6, CH	4.98, m	11, 13	66.9, CH	3.62, m	4, 11, 13
13	176.9, qC			173.6, qC		
14	16.2, CH_2	2.67, q (7.5)	6, 7, 8, 15	15.5, CH_2	2.55, m	6, 7, 8, 15
15	13.4, CH_3	1.09, t (7.5)	7, 14	13.3, CH_3	1.03, t (7.0)	7, 14
3-OCH_3	57.6	3.99, s	3	55.9	3.79, s	3
6-OCH_3	56.5	3.98, s	6	56.6	3.89, s	6
13-OCH_3				51.6	3.51, s	13
OH-4					6.13, s	4, 10, 11
OH-8		13.14, s	7, 8, 9		13.29, s	7, 8, 9
OH-12		5.30, d (6.0)	11, 12, 13		5.24, d (6.5)	11, 12, 13

[a]Recorded at 125 MHz in acetone-d_6. [b]Recorded at 500 MHz in acetone-d_6. [c]Recorded at 125 MHz in DMSO-d_6. [d]Recorded at 500 MHz in DMSO-d_6.

α,β-unsaturated ketone carbon (δ_C 190.0). These data accounted for all the resonances observed in the NMR spectra of **1**. The $^1H-^1H$ COSY NMR data of **1** showed the isolated spin systems of C-11−C-12 (including OH-12) and C-14−C-15. HMBC correlations from H_3-15 to C-7, from H_2-14 to C-6 and C-8, and from H-5 to C-6, C-7, C-9, and C-10, together with those from the intramolecularly hydrogen-bonded phenolic proton OH-8 to C-7 and C-9, established a pentasubstituted aryl ring with an ethyl and a hydroxy group attached to C-7 and C-8, respectively. HMBC cross-peaks from H-2 to C-1, C-3, C-4, and C-9 revealed the connectivities of the C-1−C-3 α,β-unsaturated ketone moiety to C-9 of the aryl ring via C-1, and the C-2/C-3 olefin to the sp^3 quaternary carbon C-4, respectively. An HMBC correlation from H-5 to C-4 established a cyclohexenone unit that was fused to the aryl ring at C-9/C-10, completing the naphthalen-1(4*H*)-one partial structure. The correlations from H-11 to C-3, C-4, C-10, and C-13 led to the connections of C-4 to C-11 and C-12 to C-13, respectively. Considering the chemical shifts of C-4 (δ_C 78.6) and C-13 (δ_C 176.9) and the unsaturation requirement of **1**, the two carbons should be attached to the remaining oxygen atom to form a γ-lactone ring, which is spirally joined to the naphthalen-1(4*H*)-one moiety at C-4, leading to assignment of the 3*H*,4′*H*-spiro[furan-2,1′-naphthalene]-4′,5(4*H*)-dione skeleton of **1**. On the basis of these data, the planar structure of **1** was established as shown.

The relative configuration of **1** was determined by X-ray crystallographic analysis, and a perspective ORTEP plot is shown in Figure 1. The absolute configuration of **1** was deduced by comparison of the experimental and simulated electronic circular dichroism (ECD) spectra generated by time-dependent density functional theory (TDDFT)[14] for enantiomers (4*R*,12*R*)-**1** (**1a**) and (4*S*,12*S*)-**1** (**1b**). A systematic conformational analysis was performed for **1a** and **1b** by the Molecular Operating Environment (MOE) software package

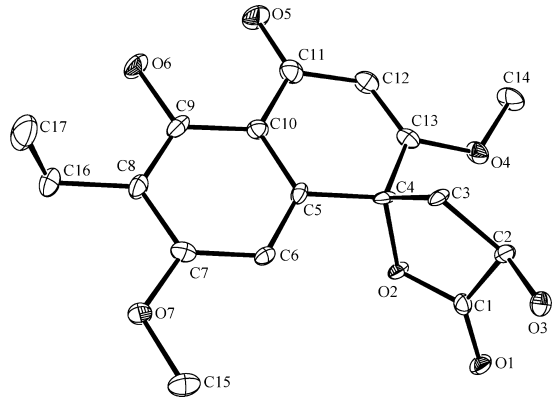

Figure 1. Thermal ellipsoid representation of **1**. (Note: A different numbering system is used for the structural data deposited with the CCDC.)

using the MMFF94 molecular mechanics force field calculation. The MMFF94 conformational search followed by reoptimization using TDDFT at the B3LYP/6-31G(d) basis set level afforded two lowest energy conformers for **1a** and **1b** (Figure S24). The overall calculated ECD spectra of **1a** and **1b** were then generated by Boltzmann-weighting of the two conformers with 46.01% and 53.99% populations, respectively, by their relative free energies (Figure 2). The absolute configuration of **1** was then extrapolated by comparison of the experimental and calculated ECD spectra of **1a** and **1b** after a UV correction of 10 nm (Figure S25). The experimental CD spectrum of **1** was nearly identical to the calculated ECD spectrum of (4*R*,12*R*)-**1** (**1a**), both showing negative Cotton effects (CEs) in the regions of 200−220 and 280−360 nm and positive CEs at 230−260 nm (Figure 2). Therefore, **1** was deduced to have the 4*R*, 12*R* absolute configuration.

dx.doi.org/10.1021/np300263u | *J. Nat. Prod.* 2012, 75, 1339−1345

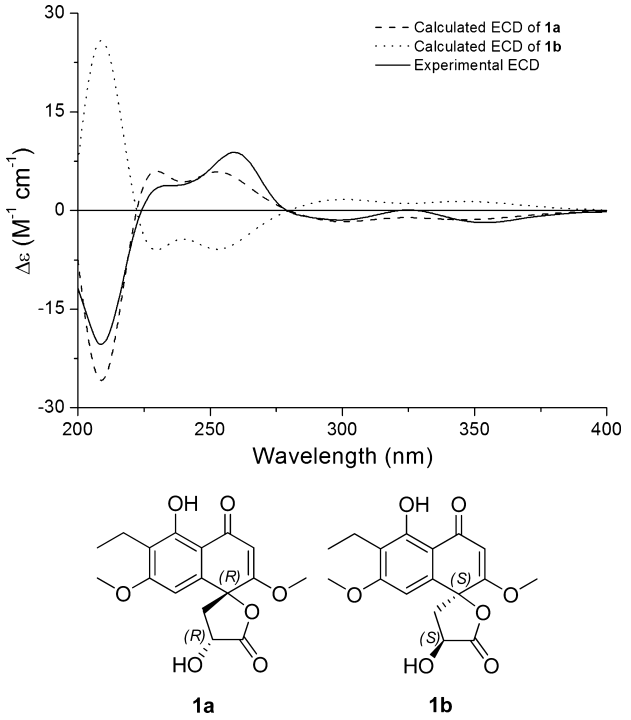

Figure 2. Experimental CD spectrum of **1** in MeOH and the calculated ECD spectra of (4*R*,12*R*)-**1** (**1a**) and (4*S*,12*S*)-**1** (**1b**) after a UV correction of 10 nm.

Perenniporide B (**2**) gave a pseudomolecular ion $[M + H]^+$ by HRESIMS, consistent with the molecular formula $C_{18}H_{22}O_8$ (eight degrees of unsaturation). Analysis of its NMR data (Table 1) revealed the same naphthalen-1(4*H*)-one partial structure as found in **1**. Additional NMR resonances corresponding to an *O*-methyl group (δ_H/δ_C 3.51/51.6) and an exchangeable proton (δ_H 6.13) were observed in the spectra of **2**, implying that the lactone unit found in **1** was absent. HMBC correlations from the exchangeable proton at 6.13 ppm to C-4, C-10, and C-11 located the hydroxy group at C-4, whereas that from the *O*-methyl proton signal to the carboxylic carbon at 173.6 ppm suggested the presence of the C-13 methyl ester. Therefore, the planar structure of **2** was determined as shown.

The absolute configuration of **2** was also deduced by comparison of the experimental and calculated ECD spectra generated for enantiomers (4*S*,12*R*)-**2**, (4*R*,12*S*)-**2**, (4*R*,12*R*)-**2**, and (4*S*,12*S*)-**2** (**2a**–**d**; Figure 3). The MMFF94 conformational search followed by B3LYP/6-31G(d) DFT reoptimization afforded 10 lowest energy conformers for enantiomers **2a** and **2b** and eight for **2c** and **2d**, respectively (Figures S26 and S27). The calculated ECD spectra of enantiomers **2a**–**d** were then generated by Boltzmann-weighting of the conformers (Figure 3). The experimental CD spectrum of **2** is comparable only to the calculated ECD curve of **2c**. Therefore, the absolute configuration of **2** was deduced to be 4*R*, 12*R*.

Perenniporide C (**3**) was assigned the same molecular formula, $C_{18}H_{22}O_8$, as **2** by HRESIMS. Interpretation of its NMR data (Table 2) showed the presence of a pentasubstituted aryl ring with the same substitution pattern and substituents as found in **1** and **2**. HMBC cross-peaks from H_2-2 to C-1, C-3, C-4, and C-9 and from H-5 to C-4 and C-10 established a cyclohexanone unit fused to the aryl ring at C-9/C-10, completing the 3,4-dihydronaphthalen-1(2*H*)-one moiety. In turn, correlations from the exchangeable proton at 5.78 ppm to C-3, C-4, C-10, and C-11 indicated that a free hydroxy group and C-11 both attach to C-4. Further cross-peaks from H_2-11 and H-12 to the carboxylic carbon at 171.8 ppm connected C-12 to C-13. An HMBC correlation from H-12 to C-3 completed a tetrahydrofuran (THF) ring fused to the 3,4-dihydronaphthalen-1(2*H*)-one moiety at C-3/C-4. Finally, the two methoxys were located at C-3 and C-13, respectively, on the basis of relevant HMBC correlations to establish the planar structure of **3**.

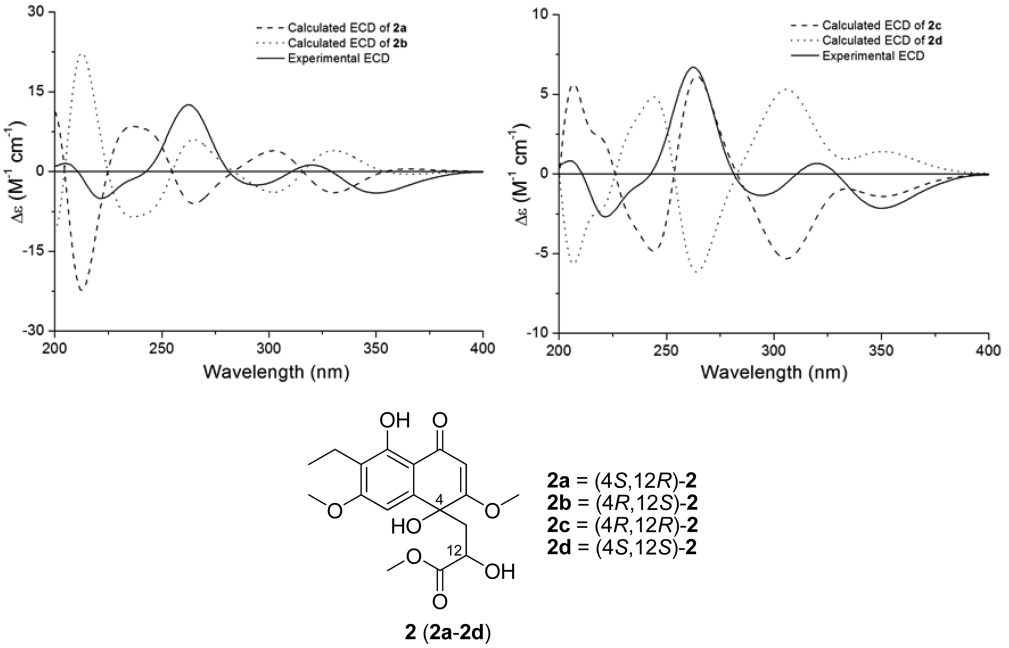

Figure 3. Experimental CD spectrum of **2** in MeOH and the calculated ECD spectra of **2a**–**d**. Structures **2a**–**d** represent four possible stereoisomers of **2**.

dx.doi.org/10.1021/np300263u | *J. Nat. Prod.* 2012, 75, 1339–1345

Table 2. NMR Data for 3 and 4

	3			4		
pos.	δ_C,[a] mult.	δ_H[b] (J in Hz)	HMBC[c]	δ_C,[c] mult.	δ_H[d] (J in Hz)	HMBC[c]
1	197.8, qC			199.8, qC		
2	41.5, CH_2	3.18, d (17.0); 3.05, d (17.0)	1, 3, 4, 9	40.4, CH_2	3.21, d (17.0); 3.03, d (17.0)	1, 3, 4, 9
3	105.8, qC			104.6, qC		
4	78.3, qC			77.9, qC		
5	102.4, CH	6.82, s	1, 4, 6, 7, 9, 10	102.9, CH	6.83, s	1, 4, 6, 7, 9, 10
6	164.1, qC			163.2, qC		
7	119.7, qC			117.0, qC		
8	160.9, qC			159.1, qC		
9	109.6, qC			109.6, qC		
10	142.7, qC			146. 4, qC		
11	43.3, CH_2	2.86, dd (13.0, 9.5); 2.76, dd (13.0, 3.5)	3, 4, 10, 12, 13	41.5, CH_2	2.83, dd (12.5, 9.5); 2.74, dd (12.5, 3.5)	3, 4, 10, 12, 13
12	74.8, CH	4.63, dd (9.5, 3.5)	3, 4, 11, 13	72.3, CH	4.49, dd (9.5, 3.5)	11, 13
13	171.8, qC			172.1, qC		
14	15.8, CH_2	2.56, q (7.0)	6, 7, 8, 15	15.2, CH_2	2.75, q (7.0)	6, 7, 8, 15
15	13.1, CH_3	0.98, t (7.0)	7, 14	13.2, CH_3	1.02, t (7.0)	7, 14
3-OCH_3	50.2	3.30, s	3	48.8	3.33, s	3
6-OCH_3	56.0	3.89, s	6	56.1	3.89, s	6
13-OCH_3	52.4	3.34, s	13			
OH-4		5.78, s	3. 4, 10, 11		5.73, s	3, 4, 10, 11
OH-8		12.66, s	7, 8, 9		12.68, s	7, 8, 9
OH-12					5.77, s	

[a]Recorded at 125 MHz in $CDCl_3$. [b]Recorded at 500 MHz in DMSO-d_6. [c]Recorded at 125 MHz in DMSO-d_6. [d]Recorded at 500 MHz in DMSO-d_6.

The absolute configuration of the C-3 oxygenated sp^3 quaternary carbon in **3** was assigned using Snatzke's sector rule for the nonplanar enones (Figure 4).[15,16] The positive CE

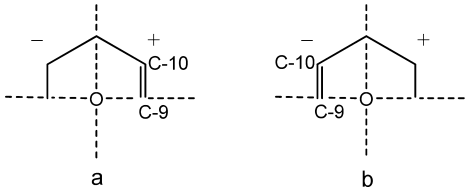

Figure 4. Application of Snatzke's enone sector rule for prediction of the sign of the n → π^* transition in the CD spectra (320−350 nm) of **3** (a) and **4** (b).

observed in the 320−350 nm (R band) region of the CD spectrum (Figure S21) suggested the 3*R* absolute configuration. A NOESY correlation of H-12 with 3-OCH_3 placed these protons on the same face of the THF ring, allowing assignment of the 12*R* absolute configuration. The absolute configuration of the C-4 tertiary alcohol was deduced by the CD data of the *in situ* formed $[Rh_2(OCOCF_3)_4]$ complex,[17] with the inherent contribution subtracted. The Rh complex of **3** showed a negative E band at ca. 350 nm (Figure S23), correlating to the 4*R* absolute configuration on the basis of the bulkiness rule.[17,18] The above assignment was supported by the ECD calculations for four stereoisomers, (3*R*,4*R*,12*R*)-**3**, (3*S*,4*S*,12*S*)-**3**, (3*R*,4*S*,12*R*)-**3**, and (3*S*,4*R*,12*S*)-**3** (**3a**−**d**; Figures S29−S31). The overall pattern of the experimental CD spectrum of **3** matched only the calculated ECD curve of **3a** (Figure 5), suggesting the 3*R*, 4*R*, 12*R* absolute configuration.

The molecular formula of perenniporide D (**4**) was determined to be $C_{17}H_{20}O_8$ (eight degrees of unsaturation) by HRESIMS. The NMR data of **4** (Table 2) revealed the same 3,4-dihydronaphthalen-1(2*H*)-one moiety as found in **3**. However, the methoxy group attached to C-13 (δ_H/δ_C 3.34/52.4) in **3** was absent, and an additional exchangeable proton was observed at 5.77 ppm, which was located at C-12 on the basis of $^1H-^1H$ COSY data. Considering the chemical shifts of C-3 (δ_C 104.6) and C-13 (δ_C 172.1), as well as the unsaturation requirement of **4**, the two carbons were both attached to the remaining oxygen atom to form a δ-lactone unit fused to the 3,4-dihydronaphthalen-1(2*H*)-one moiety at C-3/C-4. These data permitted the assignment of the planar structure of **4**.

The absolute configuration of the C-3 oxygenated sp^3 quaternary carbon in **4** was also deduced using Snatzke's enone sector rule[15,16] and Klyne's sector lactone rule (Figure 6).[15] The CD spectrum of **4** (Figure S22) showed negative CEs in the 320−350 (R band) and 210−220 nm regions, correlating to the 3*S* and 4*R* absolute configurations, respectively. A ROESY correlation of H-12 with 3-OCH_3 revealed the 12*R* absolute configuration. The above assignment was supported by the ECD calculations for two stereoisomers, (3*S*,4*R*,12*R*)-**4** and (3*R*,4*S*,12*S*)-**4** (**4a** and **4b**; Figures S32 and S33). The overall pattern of the experimental CD spectrum of **4** matched the calculated ECD curve of **4a** proportionally (Figure 7), suggesting the 3*S*, 4*R*, 12*R* absolute configuration. Therefore, the absolute configuration of **4** was deduced to be 3*S*, 4*R*, 12*R*.

The known compound **5** was identified as 6-ethyl-2,7-dimethoxyjuglone by comparison of its NMR and MS data with those reported.[13]

Compounds **1**−**4** were tested for their antifungal activity against a panel of five plant pathogens, including *Fusarium moniliforme* (CGMCC 3.2835), *Verticillium albo-atrum* (CGMCC 3.4306), *Gibberella zeae* (CGMCC 3.2873), *Fusarium oxysporum* (CGMCC 3.2830), and *Alternaria longipes* (CGMCC 3.2875). Compound **1** showed a significant inhibitory effect against the five pathogens, with MIC values of 20, 20, 20, 10, and 10 μg/mL, respectively. The positive control methyl 2-benzimidazolecarbamate showed antifungal activity against all the tested pathogens except *A. longipes*, with

dx.doi.org/10.1021/np300263u | *J. Nat. Prod.* 2012, 75, 1339−1345

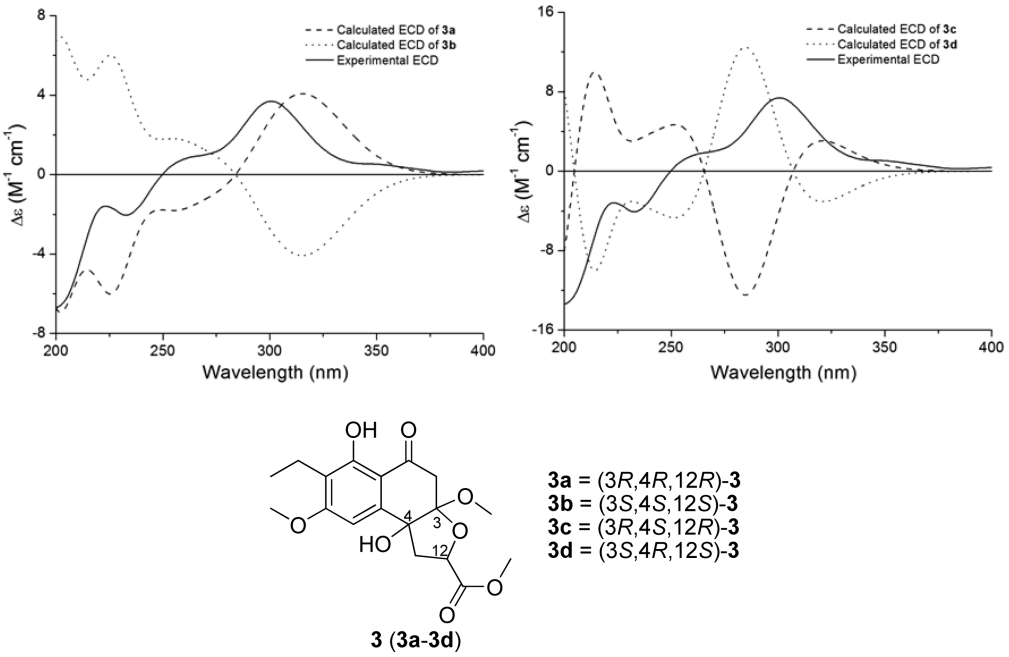

Figure 5. Experimental CD spectrum of **3** in MeOH and the calculated ECD spectra of **3a**–**d**. Structures **3a**–**d** represent four possible stereoisomers of **3**.

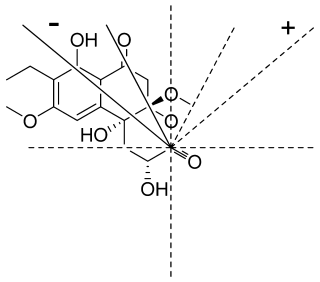

Figure 6. Application of Klyne's sector lactone rule viewed from above for prediction of the sign of the n → π^* transition in the CD spectrum (210–220 nm) of **4**.

MIC values of 0.63, 0.63, 2.5, and 0.63 μg/mL, respectively, whereas **2**–**4** did not show detectable activity at 20 μg/mL.

Although perenniporide A (**1**) is structurally related to a synthetic intermediate (**6**) of the pseudopterosins,[19,20] it is the first naturally occurring naphthalenone with the 3′,4′-dihydro-2′*H*,3*H*-spiro[furan-2,1′-naphthalen]-5(4*H*)-one skeleton. Compound **2** is analogous to the known compound **7** produced by *Guignardia laricina*, a causative fungus of larch shoot blight,[21] but differs by having a different substituent at C-4. Compound **3** has the relatively rare 1,2,3a,4-tetrahydronaphtho[2,1-*b*]furan-5(9b*H*)-one skeleton, with fungal metabolite strobilol H (**8**)[22,23] as its closely related natural product. Compound **4** represents the first natural product with the 4a,5,6,10b-tetrahydro-1*H*-benzo[*f*]chromen-3(2*H*)-one skeleton, which was previously found only in synthetic compounds (e.g., **9**).[24] Biogenetically, compounds **1**–**4** could be generated from the co-isolated known compound **5** via different routes, as illustrated in the hypothetical biosynthetic pathways (Scheme S1).

EXPERIMENTAL SECTION

General Experimental Procedures. Optical rotations were measured on a Perkin-Elmer 241 polarimeter, and UV data were obtained on a Shimadzu Biospec-1601 spectrophotometer. CD spectra were recorded on a JASCO J-815 spectropolarimeter. IR data were recorded using a Nicolet Magna-IR 750 spectrophotometer. ^{1}H and ^{13}C NMR data were acquired with Inova-500 and NMR system-600 spectrometers using solvent signals (acetone-d_6: δ_H 2.05/δ_C 29.8, 206.1; DMSO-d_6: δ_H 2.50/δ_C 39.5; $CDCl_3$: δ_H 7.26/δ_C 77.2) as references. The HMQC and HMBC experiments were optimized for 145.0 and 8.0 Hz, respectively. ESIMS and HRESIMS data were obtained using an Agilent Accurate-Mass-Q-TOF LC/MS 6520 instrument equipped with an electrospray ionization (ESI) source.

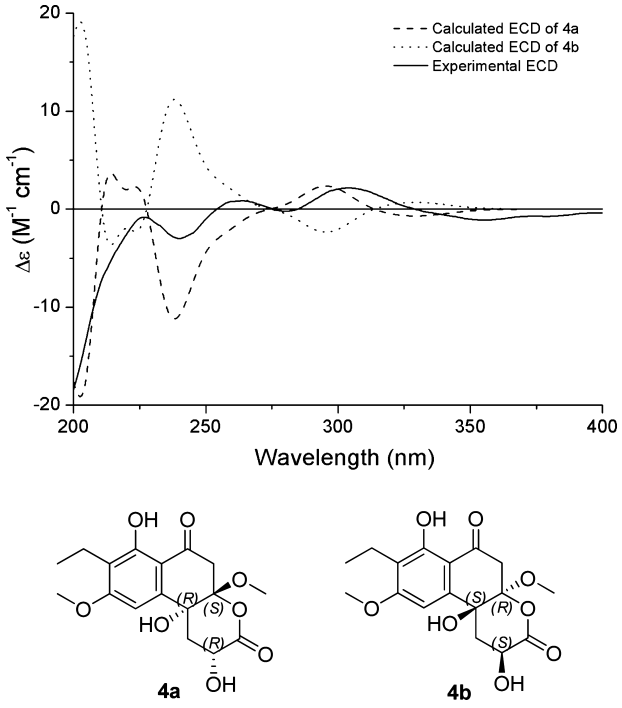

Figure 7. Experimental CD spectrum of **4** in MeOH and the calculated ECD spectra of **4a** and **4b**. Structures **4a** and **4b** represent two possible stereoisomers of **4**.

dx.doi.org/10.1021/np300263u | *J. Nat. Prod.* 2012, 75, 1339–1345

The fragmentor and capillary voltages were kept at 125 and 3500 V, respectively. Nitrogen was supplied as the nebulizing and drying gas. The temperature of the drying gas was set at 300 °C. The flow rate of the drying gas and the pressure of the nebulizer were 10 L/min and 10 psi, respectively. All MS experiments were performed in positive ion mode. Full-scan spectra were acquired over a scan range of m/z 100−1000 at 1.03 spectra/s. HPLC separations were performed on an Agilent 1200 instrument (Agilent, USA) equipped with a variable-wavelength UV detector.

Fungal Material. The culture of *Perenniporia* sp. was isolated from the larva of *Euops chinesis* collected from Mingyue Mountain, Jiangxi Province, People's Republic of China, in October 2010. The isolate was identified by one of the authors (L.W.) on the basis of morphology and sequence (GenBank accession no. JQ348934) analysis of the ITS region of the rDNA. The fungal strain was cultured on slants of potato dextrose agar (PDA) at 25 °C for 10 days. Agar plugs were cut into small pieces (about 0.5 × 0.5 × 0.5 cm^3) under aseptic conditions; 15 pieces were used to inoculate three Erlenmeyer flasks (250 mL), each containing 50 mL of media (0.4% glucose, 1% malt extract, and 0.4% yeast extract; the final pH of the media was adjusted to 6.5 and sterilized by autoclave). Three flasks of the inoculated media were incubated at 25 °C on a rotary shaker at 170 rpm for five days to prepare the seed culture. Fermentation was carried out in 12 Fernbach flasks (500 mL), each containing 80 g of rice. Distilled H_2O (120 mL) was added to each flask, and the contents were soaked overnight before autoclaving at 15 psi for 30 min. After cooling to room temperature, each flask was inoculated with 5.0 mL of the spore inoculum and incubated at 25 °C for 40 days.

Extraction and Isolation. The fermented material was extracted repeatedly with EtOAc (4 × 1.0 L), and the organic solvent was evaporated to dryness under vacuum to afford the crude extract (5.0 g), which was fractionated by silica gel VLC using CH_2Cl_2−MeOH gradient elution. The fraction (300 mg) eluted with CH_2Cl_2 was separated again by Sephadex LH-20 column chromatography (CC) using 1:1 CH_2Cl_2−MeOH as eluents, and the resulting subfractions were further purified by semipreparative RP HPLC (Agilent Zorbax SB-C_{18} column; 5 μm; 9.4 × 250 mm; 60−100% MeOH in H_2O over 30 min; 2 mL/min) to afford **5** (50.0 mg, t_R 23.55 min). The fractions (1.2 g) eluted with 1% and 2% MeOH were combined and separated by Sephadex LH-20 CC eluting with MeOH. The resulting subfractions were purified by RP HPLC to afford **2** (4.3 mg, t_R 9.04 min; 50% CH_3CN in H_2O for 30 min), **3** (31.1 mg, t_R 14.78 min; the same gradient as in purification of **2**), **1** (107.9 mg, t_R 17.11 min; the same gradient as in purification of **2**), and **4** (7.8 mg, t_R 35.63 min; 25−33% CH_3CN in H_2O over 30 min, followed by 33−70% over 50 min).

Perenniporide A (1): pale yellow powder; $[\alpha]^{25}_D$ +11.7 (*c* 0.34, MeOH); UV (MeOH) λ_{max} (log ε) 229 (3.92), 256 (3.99), 340 (3.74) nm; CD (*c* 6.0 × 10^{-4} M, MeOH) λ_{max} ($\Delta\varepsilon$) 209 (−10.84), 259 (+4.72), 299 (−0.71), 354 (−0.98) nm; IR (neat) ν_{max} 3329 (br), 2941, 2875, 1792, 1646, 1608, 1458, 1322, 1242, 1132 cm^{-1}; ^1H, ^{13}C NMR and HMBC data see Table 1; HRESIMS m/z 335.1124 (calcd for $C_{17}H_{19}O_7$, 335.1125).

X-ray Crystallographic Analysis of 1 (ref 25). Upon crystallization from acetone using the vapor diffusion method, pale yellow crystals of **1** were obtained. A crystal (0.30 × 0.20 × 0.20 mm) was separated from the sample and mounted on a glass fiber, and data were collected using a Rigaku RAXIS RAPID IP diffractometer with graphite-monochromated Mo Kα radiation, λ = 0.71073 Å at 123(2) K. Crystal data: $C_{17}H_{18}O_7$, M = 334.31, space group orthorhombic, $P2(1)2(1)2(1)$; unit cell dimensions a = 6.2340(12) Å, b = 11.064 (2) Å, c = 22.677 (5) Å, V = 1564.1 (5) $Å^3$, Z = 4, D_{calcd} = 1.420 mg/m^3, μ = 0.111 mm^{-1}, $F(000)$ = 704. The structure was solved by direct methods using SHELXL-97[26] and refined by using full-matrix least-squares difference Fourier techniques. All non-hydrogen atoms were refined with anisotropic displacement parameters, and all hydrogen atoms were placed in idealized positions and refined as riding atoms with the relative isotropic parameters. Absorption corrections were performed using the Siemens Area Detector Absorption Program (SADABS).[27] The 9082 measurements yielded 3592 independent reflections after equivalent data were averaged, and Lorentz and polarization corrections were applied. The final refinement gave R_1 = 0.0387 and wR_2 = 0.0717 [$I > 2\sigma(I)$].

Perenniporide B (2): colorless oil; $[\alpha]^{25}_D$ −23.0 (*c* 0.10, MeOH); UV (MeOH) λ_{max} (log ε) 207 (3.07), 256 (2.77), 335 (2.56) nm; CD (*c* 5.5 × 10^{-4} M, MeOH) λ_{max} ($\Delta\varepsilon$) 205 (+0.82), 222 (−2.68), 263 (+6.70), 295 (−1.35), 320 (+0.66), 350 (−2.15) nm; IR (neat) ν_{max} 3440 (br), 2966, 1742, 1639, 1609, 1420, 1314, 1238, 1136 cm^{-1}; ^1H, ^{13}C NMR and HMBC data see Table 1; HRESIMS m/z 367.1401 (calcd for $C_{18}H_{23}O_8$, 367.1387).

Perenniporide C (3): colorless oil; $[\alpha]^{25}_D$ −38.9 (*c* 0.09, MeOH); UV (MeOH) λ_{max} (log ε) 231 (3.96), 288 (3.90) nm; CD (*c* 2.7 × 10^{-4} M, MeOH) λ_{max} ($\Delta\varepsilon$) 223 (−1.19), 233 (−1.53), 263 (+0.66), 301 (+2.77), 350 (+0.40), 386 (+0.09) nm; IR (neat) ν_{max} 3486 (br), 2966, 2875, 1737, 1629, 1575, 1459, 1298, 1134, 1051 cm^{-1}; ^1H, ^{13}C NMR and HMBC data see Table 2; NOESY data (acetone-d_6, 500 MHz) H-5 ↔ H_2-14, H-5 ↔ 6-OCH_3, H-12 ↔ 3-OCH_3; HRESIMS m/z 367.1407 (calcd for $C_{18}H_{23}O_8$, 367.1387).

Absolute Configuration of the C-4 Tertiary Alcohol in 3 (refs 17 and 18). A sample of **1** (1.0 mg) was dissolved in a dry solution of [$Rh_2(OCOCF_3)_4$] complex (1.7 mg) in CH_2Cl_2 (1.0 mL). The first CD spectrum was recorded immediately after mixing, and its time evolution was monitored until stationary (ca. 10 min after mixing). The inherent CD was subtracted. The observed sign of the E band at ca. 350 nm in the induced CD spectrum was correlated to the absolute configuration of the C-4 tertiary alcohol moiety.

Perenniporide D (4): colorless oil; $[\alpha]^{25}_D$ −23.0 (*c* 0.10, MeOH); UV (MeOH) λ_{max} (log ε) 223 (3.93), 238 (3.99), 288 (3.94), 330 (3.74) nm; CD (*c* 5.7 × 10^{-4} M, MeOH) λ_{max} ($\Delta\varepsilon$) 227 (−0.14), 240 (−0.50), 264 (+0.14), 305 (+0.36), 356 (−0.19) nm; IR (neat) ν_{max} 3452 (br), 2936, 1732, 1631, 1418, 1302, 1238, 1135, 1051 cm^{-1}; ^1H, ^{13}C NMR and HMBC data see Table 2; ROESY data (DMSO-d_6, 500 MHz) H-5 ↔ H_2-14, H-5 ↔ H_2-11, H-5 ↔ 6-OCH_3, H-12 ↔ 3-OCH_3; HRESIMS m/z 353.1231 (calcd for $C_{17}H_{21}O_8$, 353.1231).

6-Ethyl-2,7-dimethoxyjuglone (5). ^1H NMR and the MS data were consistent with literature values.[13]

Computational Details. Systematic conformational analyses for **1**, **2**, and **3** were performed via the Molecular Operating Environment ver. 2009.10 (Chemical Computing Group, Canada) software package using the MMFF94 molecular mechanics force field calculation. The MMFF94 conformational analyses were further optimized using TDDFT at the B3LYP/6-31G(d) basis set level. The stationary points have been checked as the true minima of the potential energy surface by verifying they do not exhibit vibrational imaginary frequencies. The 30 lowest electronic transitions were calculated, and the rotational strengths of each electronic excitation were given using both dipole length and dipole velocity representations. ECD spectra were stimulated using a Gaussian function with a half-bandwidth of 0.3 eV. Equilibrium populations of conformers at 298.15 K were calculated from their relative free energies (ΔG) using Boltzmann statistics. The overall ECD spectra were then generated according to Boltzmann-weighting of each conformer. The systematic errors in the prediction of the wavelength and excited-state energies are compensated for by employing UV correlation. All quantum computations were performed using the Gaussian03 package[28] on an IBM cluster machine located at the High Performance Computing Center of Peking Union Medical College.

Antifungal Assays. Antifungal assays were conducted in triplicate following National Center for Clinical Laboratory Standards (NCCLS) recommendations.[29] The plant pathogens, *A. longipes* (CGMCC 3.2875), *F. moniliforme* (CGMCC 3.2835), *V. albo-atrum* (CGMCC 3.4306), *G. zeae* (CGMCC 3.2873), and *F. oxysporum* (CGMCC 3.2830), were obtained from China General Microbial Culture Collection (CGMCC) and were grown on PDA. Targeted fungi (3 or 4 colonies) were prepared from broth cultures incubated at 28 °C for 48 h, and the final suspensions contained 10^4 hyphae/mL (in PDB medium). Test samples (10 mg/mL as stock solution in DMSO and serial dilutions) were transferred to 96-well clear plates in triplicate, and the suspensions of the test organisms were added to each well to achieve a final volume of 200 μL with Alamar blue (10 μL

of 10% solution) added to each well as indicator. After incubation at 28 °C for 48 h, the fluorescence intensity was measured at Ex/Em = 544/590 nm using a microtiter plate reader. The inhibition rates were calculated and plotted versus the test concentrations to afford the MICs, which were defined as the lowest concentration that completely inhibited the growth of the test organisms.

■ ASSOCIATED CONTENT

Supporting Information

^{1}H, ^{13}C, and 2D NMR spectra of **1**−**4**, CD spectra of **3** and **4**, Rh complex of **3**, and UV and CD calculations for **1**−**4**. This material is available free of charge via the Internet at http://pubs.acs.org.

■ AUTHOR INFORMATION

Corresponding Author

*Tel/Fax: +86 10 82618785. E-mail: (Y.C.) cheys@im.ac.cn; (X.L.) liuxz@im.ac.cn.

Author Contributions

§These authors contributed equally to this work.

Notes

The authors declare no competing financial interest.

■ ACKNOWLEDGMENTS

We gratefully acknowledge financial support from the National Natural Science Foundation of China (30925039), Beijing Natural Science Foundation (5111003), the Ministry of Science and Technology of China (2010ZX09401-403 and 2012ZX09301-003), and the Chinese Academy of Sciences (KSCX2-EW-G-6).

■ REFERENCES

(1) Sakurai, K. *J. Ethol.* **1985**, *3*, 151−156.

(2) (a) Hu, H.; Guo, H.; Li, E.; Liu, X.; Zhou, Y.; Che, Y. *J. Nat. Prod.* **2006**, *69*, 1672−1675. (b) Guo, H.; Hu, H.; Liu, S.; Liu, X.; Zhou, Y.; Che, Y. *J. Nat. Prod.* **2007**, *70*, 1519−1521. (c) Li, Y.; Sun, B.; Liu, S.; Jiang, L.; Liu, X.; Zhang, H.; Che, Y. *J. Nat. Prod.* **2008**, *71*, 1643−1646. (d) Li, Y.; Ye, D.; Chen, X.; Lu, X.; Shao, Z.; Zhang, H.; Che, Y. *J. Nat. Prod.* **2009**, *72*, 912−916. (e) Wang, Y.; Zheng, Z.; Liu, S.; Zhang, H.; Li, E.; Guo, L.; Che, Y. *J. Nat. Prod.* **2010**, *73*, 920−924. (f) Liu, L.; Niu, S.; Lu, X.; Chen, X.; Zhang, H.; Guo, L.; Che, Y. *Chem. Commun.* **2010**, *46*, 460−462. (g) Li, J.; Li, L.; Si, Y.; Jiang, X.; Guo, L.; Che, Y. *Org. Lett.* **2011**, *13*, 2670−2673. (h) Zhang, F.; Li, L.; Niu, S.; Si, Y.; Guo, L.; Jiang, X.; Che, Y. *J. Nat. Prod.* **2012**, *75*, 230−237.

(3) Murrill, W. A. *Mycologia* **1942**, *34*, 595−596.

(4) Kida, T.; Shibai., H; Seto, H. *J. Antibiot.* **1986**, *39*, 613−615.

(5) Hirotani, M.; Ino, C.; Furuya, T.; Shirot, M. *Phytochemistry* **1984**, *23*, 1129−1134.

(6) Hirotani, M.; Ino, C.; Furuya, T.; Shirot, M. *Phytochemistry* **1984**, *23*, 2885−2888.

(7) Kida, T.; Shibai, H.; Seto, H. Japanese Patent 62123194, 1987.

(8) Tsukida, K.; Yoneshige, M. *Yakugaku Zasshi* **1954**, *74*, 379−382.

(9) Kimura, Y.; Kozawa, M.; Baba, K.; Hata, K. *Planta Med.* **1983**, *48*, 164−168.

(10) Kubo, M.; Kimura, Y.; Shin, H.; Haneda, T.; Tani, T.; Namba, K. *Shoyakugaku Zasshi* **1981**, *35*, 58−61.

(11) Jayatilake, G. S.; Jayasuriya, H.; Lee, E. S.; Koonchanok, N. M.; Geahlen, R. L.; Ashendel, C. L.; McLaughlin, J. L.; Chang, C. J. *J. Nat. Prod.* **1993**, *56*, 1805−1810.

(12) Kuznetsova, Z. P. *Vesti Akad. Navuk BSSR, Ser. Biyal. Navuk* **1979**, *5*, 29−32.

(13) Poch, G. K.; Gloer, J. B.; Shearer, C. A. *J. Nat. Prod.* **1992**, *55*, 1093−1099.

(14) (a) Diedrich, C.; Grimme, S. *J. Phys. Chem. A* **2003**, *107*, 2524−2539. (b) Crawford, T. D.; Tam, M. C.; Abrams, M. L. *J. Phys. Chem. A* **2007**, *111*, 12058−12068. (c) Stephens, P. J.; Devlin, F. J.; Gasparrini, F.; Ciogli, A.; Spinelli, D.; Cosimelli, B. *J. Org. Chem.* **2007**, *72*, 4707−4715. (d) Ding, Y.; Li, X. C.; Ferreira, D. *J. Org. Chem.* **2007**, *72*, 9010−9017. (e) Berova, N.; Bari, L. D.; Pescitelli, G. *Chem. Soc. Rev.* **2007**, *36*, 914−931. (f) Bringmann, G; Bruhn, T.; Maksimenka, K.; Hemberger, Y. *Eur. J. Org. Chem.* **2009**, *17*, 2717−2727.

(15) Minkin, V. I.; Legrand, M.; Rougier, M. J. *Stereochemistry*, Vol. 2; Georg Thieme Publishers, 1977; pp 123−141.

(16) Snatzke, G. *Tetrahedron* **1965**, *21*, 413−419.

(17) Frelek, J.; Szczepek, W. J. *Tetrahedron: Asymmetry* **1999**, *10*, 1507−1520.

(18) Gerards, M.; Snatzke, G. *Tetrahedron: Asymmetry* **1990**, *1*, 221−236.

(19) Harrowven, D. C.; Wilden, J. D.; Tyte, M. J.; Hursthouse, M. B.; Coles, S. J. *Tetrahedron Lett.* **2001**, *42*, 1193−1195.

(20) Harrowven, D. C.; Tyte, M. J. *Tetrahedron Lett.* **2004**, *45*, 2089−2091.

(21) Otomo, N.; Sato, H.; Sakamura, S. *Agric. Biol. Chem.* **1983**, *47*, 1115−1119.

(22) Hiramatsu, F.; Murayama, T.; Koseki, T.; Okada, K.; Shiono, Y. *Helv. Chim. Acta* **2008**, *91*, 1595−1603.

(23) Hiramatsu, F.; Murayama, T.; Koseki, T.; Funakoshi, T.; Shiono, Y. *Nat. Prod. Rep.* **2011**, *25*, 781−788.

(24) Degnan, A. P.; Meyers, A. I. *J. Org. Chem.* **2000**, *65*, 3503−3512.

(25) Crystallographic data for **1** have been deposited with the Cambridge Crystallographic Data Centre (deposition number CCDC 871014). Copies of the data can be obtained, free of charge, on application to the director, CCDC, 12 Union Road, Cambridge CB2 1EZ, UK (fax: +44 1223 336033 or e-mail: deposit@ccdc.cam.ac.uk).

(26) Sheldrick, G. M. *SHELXL-97, Program for X-ray Crystal Structure Solution and Refinement*; University of Göttingen: Göttingen, Germany, 1997.

(27) Sheldrick, G. M. *SADABS, Program for Empirical Absorption Correction of Area Detector Data*; University of Göttingen: Göttingen, Germany, 1999.

(28) Frisch, M. J.; Trucks, G. W.; Schlegel, H. B.; Scuseria, G. E.; Robb, M. A.; Cheeseman, J. R.; Montgomery, J. A., Jr.; Vreven, T.; Kudin, K. N.; Burant, J. C.; Millam, J. M.; Iyengar, S. S.; Tomasi, J.; Barone, V.; Mennucci, B.; Cossi, M.; Scalmani, G.; Rega, N.; Petersson, G. A.; Nakatsuji, H.; Hada, M.; Ehara, M.; Toyota, K.; Fukuda, R.; Hasegawa, J.; Ishida, M.; Nakajima, T.; Honda, Y.; Kitao, O.; Nakai, H.; Klene, M.; Li, X.; Knox, J. E.; Hratchian, H. P.; Cross, J. B.; Bakken, V.; Adamo, C.; Jaramillo, J.; Gomperts, R.; Stratmann, R. E.; Yazyev, O.; Austin, A. J.; Cammi, R.; Pomelli, C.; Ochterski, J. W.; Ayala, P. Y.; Morokuma, K.; Voth, G. A.; Salvador, P.; Dannenberg, J. J.; Zakrzewski, V. G.; Dapprich, S.; Daniels, A. D.; Strain, M. C.; Farkas, O.; Malick, D. K.; Rabuck, A. D.; Raghavachari, K.; Foresman, J. B.; Ortiz, J. V.; Cui, Q.; Baboul, A. G.; Clifford, S.; Cioslowski, J.; Stefanov, B. B.; Liu, G.; Liashenko, A.; Piskorz, P.; Komaromi, I.; Martin, R. L.; Fox, D. J.; Keith, T.; Al-Laham, M. A.; Peng, C. Y.; Nanayakkara, A.; Challacombe, M.; Gill, P. M. W.; Johnson, B.; Chen, W.; Wong, M. W.; Gonzalez, C.; and Pople, J. A. *Gaussian 03*, Revision E. 01; Gaussian, Inc.: Wallingford, CT, 2004.

(29) NCCLS. NCCLS document M38-A; NCCLS: Wayne, PA, 2002.